AIMS Materials Science, 3(2): 404-424.
DOI: 10.3934/matersci.2016.2.404
Received: 12 February 2016
Accepted: 20 March 2016
Published: 22 March 2016

http://www.aimspress.com/journal/Materials

Short review

Some recent findings on the use of SEM-EDS in microstructural characterisation of as-sprayed and thermally aged porous coatings: a short review

Giovanni Di Girolamo [1,*], Alida Brentari [2], and Emanuele Serra [1]

[1] ENEA, SSPT-PROMAS, Casaccia Research Centre, Rome, Italy
[2] ENEA, SSPT-PROMAS, Faenza Research Centre, Faenza, Italy

* **Correspondence:** Email: giovanni.digirolamo@enea.it; Tel: +39-0630481.

Abstract: Microstructural analysis by electron microscopy techniques is a powerful tool for determining the basic and functional properties of materials and their relationship with the processing parameters, thus giving useful keys to designers and producers for optimizing performance and durability of the related components. Materials and coatings produced by thermal spraying of powder-based raw materials exhibit unique physical, thermal and mechanical properties, resulting from the thermal effects associated to their processing. These properties can be tailored depending on the application the components are addressed to. Moreover, they can change during operation because of any aging mechanisms promoted by oxidation, corrosion, thermal exposure and wear, that can be responsible of reduced performance, degradation and damage, thus affecting their durability and service lifetime. In this work, the potentiality of scanning electron microscopy (SEM) is investigated with the purpose to analyze in detail the complex microstructure and some aging effects in metallic, ceramic and composite coatings, such as formation of oxide scales, grain growth, sintering, and so on. The analysis can be successfully expanded to a wide variety of materials as well as to the study of complex mechanisms of degradation occurring during service.

Keywords: microstructure; scanning electron microscopy; aging; coatings; plasma spray

Abbreviations

3D: Three-dimensional
BSE: Backscattered Secondary Electron
EDS: Energy Dispersive Spectroscopy
FEG: Field Emission Gun
HVOF: High Velocity Oxy-Fuel
SE: Secondary Electron

SEM: Scanning Electron Microscopy
SPS: Suspension Plasma Spray
SPPS: Solution Precursor Plasma Spray
TBC: Thermal Barrier Coating

1. Introduction

The microstructural characterisation plays a key role in understanding the structure-property relationship in a lot of materials, as well as in making some predictions about the service behaviour of the related components and systems.

To this aim, scanning electron microscopy (SEM) can be a powerful tool to analyze both the morphological and microstructural features of powder-based and bulk materials, as well as the effects promoted by processing and aging on the final microstructure.

This advanced technique of analysis can be successfully employed to study the unique microstructure of coatings produced by thermal spraying, starting from powder-based materials with different size (micro or nanostructured) and morphology.

Thermal spraying processes of metallic, ceramic and composite raw materials are recognized as particularly suitable to fabricate protective coatings for multi-functional applications, such as thermal barrier coatings for blades and vanes of gas turbines, anti-oxidant coatings, anti-wear coatings for components and tools used in oil, paper and textile industries [1,2].

The thermal effects associated to the spraying process play a significant role on the final microstructure of the deposited coatings and the microstructural analysis is expected to provide a great contribution in order to detect the typical characteristics and their dependence on processing parameters, as well as their evolution during thermal exposure or at typical service conditions, depending on the operative environment and usually promoting some degradation effects associated to oxidation, corrosion, erosion and wear phenomena. These environmental effects can typically produce phase changes, sintering, degradation and damaging by delamination and spallation, reducing the performance and the durability of the whole coating system [3,4,5]. Therefore, they have to be clearly explained and possibly prevented or restricted. To this purpose, microstructural analysis provides potential support for making predictions about service behaviour and durability, as well as for characterising the state of the exposed components.

In the last years, the knowledge of the microstructure of thermally sprayed coatings has been enriched by some interesting developments in the use of X-ray micro-tomography and microstructure simulation tools for three-dimensional (3D) image analysis: the non-destructive three-dimensional image reconstruction allows to obtain detailed microstructural information on the main features of porous coatings, such as interfaces, pore shape, size, distribution, orientation and interconnection, and it is surely less time-consuming than standard microstructural investigations on serial coating cross sections. However, in any cases the limited resolution of micro-tomography does not allow to resolve the finest features, such as the small microcracks and nanopores embedded within the microstructure, that contribute to the total porosity of the coatings and then affect their thermal and mechanical properties [6–9]. In addition, there is still a lot of useful work than can be done using standards SEM-EDS analyses.

In this work, the authors present significant case studies, in order to highlight the potentiality of SEM and Energy Dispersive Spectroscopy (EDS) techniques to investigate the detailed microstructure of metallic, ceramic and composite coatings, as well as to explain the relevant aspects

related to aging and degradation at extreme operating conditions, typical of components and systems used in energy, transport and manufacturing sectors. The evolution of coating morphology and microstructure is then analyzed in detail.

2. Powder Particles & Thermal Spray Processing

Protective coatings are industrially recognized as cost-effective technological solutions for functionalizing the surface of expensive structural components, increasing their environmental resistance, temperature capability, durability, without compromising their bulk properties, thus allowing higher efficiency and lower pollution [10].

In thermal spraying a heat source is employed to melt the raw material, generally in form of powder particles and micron-sized agglomerates. These particles are fed by a carrier gas, injected in the flame/plasma jet and overheated above their melting point. The molten droplets are then propelled by the gas stream towards the substrate to be coated. Upon impact they are flattened and quenched to room temperature, thus producing the deposition of overlapped splats and, finally, the build-up of a coating with lamellar microstructure. Both the morphology and the size of the powder particles affect their melting state and then the physical, microstructural and mechanical properties of the as-deposited coatings. Many types of thermal spray equipment are available, thus enabling to process raw materials with different intrinsic physical and chemical properties that can change because of spraying temperature and environment. The temperature and the speed of the sprayed particles play a relevant role on the evolution of their properties [11]. Among various spraying systems, High Velocity Oxy Fuel (HVOF), Cold Spraying and Detonation Gun are more suitable to process materials much sensitive to thermal effects, such as metals and composites, as well as to deposit denser coatings with high bonding strength, whereas plasma spraying processes are particularly flexible and suitable to deposit high-melting point materials like ceramics for fabrication of porous coatings [12–16]. Technology enhancements are also emerging for the fabrication of nanostructured coatings, by innovative solution precursor and suspension plasma spraying (SPPS and SPS) [17,18,19].

In plasma spraying the high-temperature plasma is generated by transferring energy into an inert gas until the energy level is sufficient to ionize the gas, allowing the electrons and ions to act independently of one another. The plasma-forming gas mixture is introduced through the gun and enters the arc chamber through a gas injector that imparts a spin or vortex flow. Then it is accelerated as it expands and comes out of the nozzle [1].

Proper particle morphology and size are needed to produce powder feedstocks suitable for plasma spraying, in order to ensure high flowability and high rate of deposition. To this aim, various manufacturing processes are usually employed for powder manufacturing, to produce micron-sized particles or agglomerates of nanostructured particles to be processed. Therefore, we can have fused and crushed, spray dried, hollow particles, and so on.

The morphology can affect the melting degree and the final microstructure of the coating. Spherical particles with intrinsic porosity are recommended in the case we are going to produce coatings with high porosity, as thermal barriers, addressed to thermal insulation of metal components working in harsh environments of combustion chambers, heat exchangers and gas turbines. In turn, more dense carbide and metallic particles are suitable for fabrication of denser coatings with high oxidation and wear resistance. Carbide particles are usually blended with a matrix, to reduce any effects of thermal decomposition during processing, usually evolving in decarburization and

oxidation processes that can drastically reduce the properties of the coatings in terms of resistance to oxidation, wear and corrosion [20].

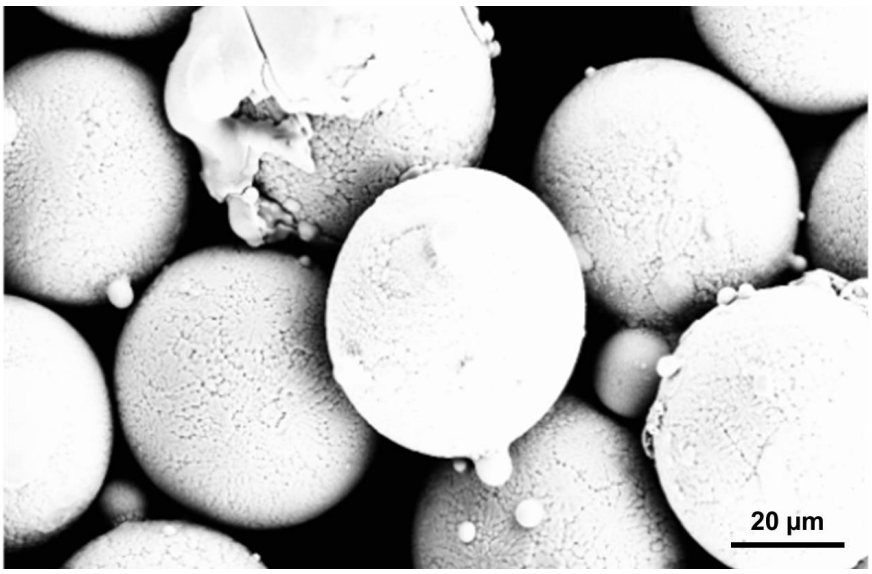

Figure 1. SEM picture showing the external morphology of CoNiCrAlYRe particles.

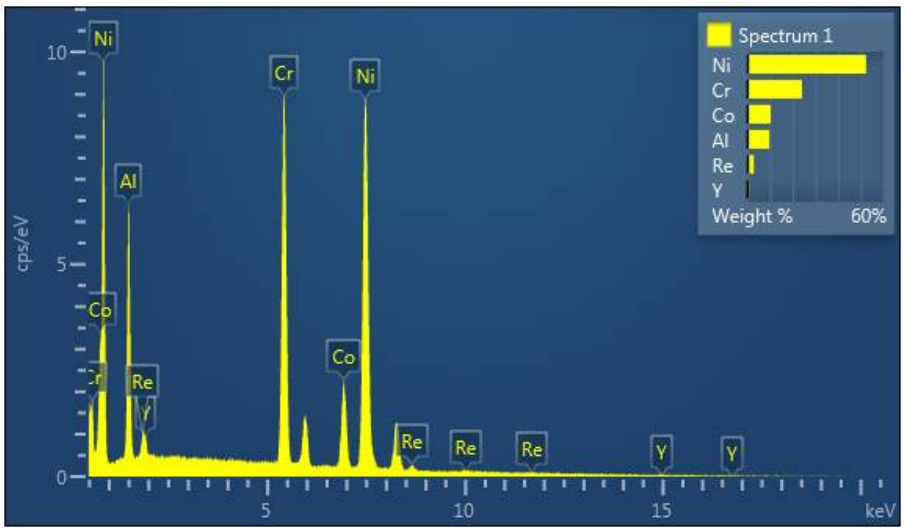

Figure 2. EDS spectrum showing the composition of CoNiCrAlYRe particle agglomerates. Reprinted with permission from [21], Di Girolamo G, Brentari A, Blasi C, et al (2014) High-temperature oxidation and oxide scale formation in plasma-sprayed CoNiCrAlYRe coatings. *Metall Mater Trans* 45A: 5362-5370, © 2014, Springer.

Figure 1 shows the morphology of spherical CoNiCrAlYRe particles. The heat transfer and the melting of the particles allow to produce coatings with good density and relatively low degree of oxidation. Figure 2 presents the EDS spectrum related to the same particles: as reported in previous study the quantitative analysis allows to calculate the elemental composition of the alloy [21]. Figure 3 shows that the external surface morphology of these particles is composed by grains with sub-micrometer size and various shape (spherical, quasi-spherical and elongated). Dendritic

structures can be also detected.

Ceramic particles generally exhibit high intrinsic porosity, as well observable in Fig. 4, which shows the morphology of spherical or quasi-spherical lanthanum zirconate powder particles for thermal barrier coating application.

The reduction of the grain size of the raw material employed is expected to provide significant enhancements in the functional properties of materials and coatings [22,23,24]. To this purpose, it is worth noting that single nanoparticles cannot be carried out by the gas stream and deposited on the substrate, because of their too low mass and momentum, so that they are usually reconstituted in micron-sized agglomerates, whose partial melting during processing allows to fabricate microstructures with unique features, *i.e.* with different morphologies, including at the same time well-melted and un-melted areas within the coating.

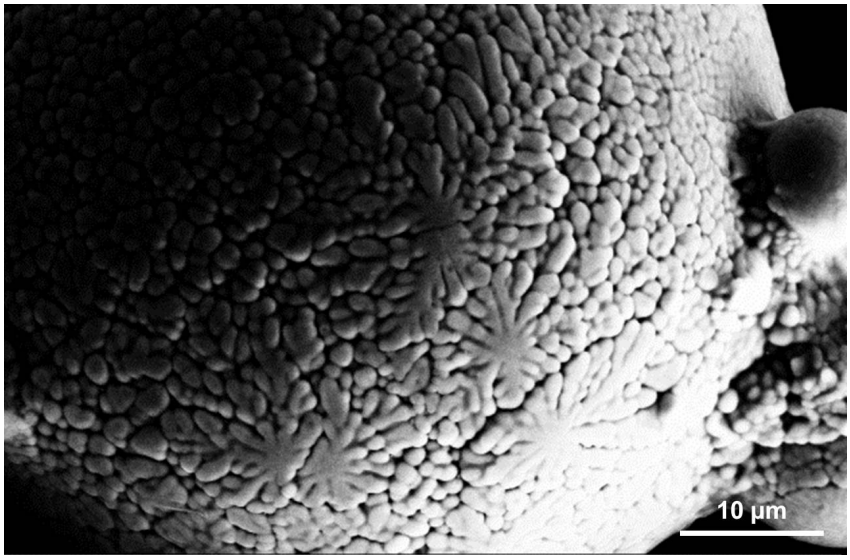

Figure 3. SEM picture showing the morphology of the external surface of CoNiCrAlYRe particle.

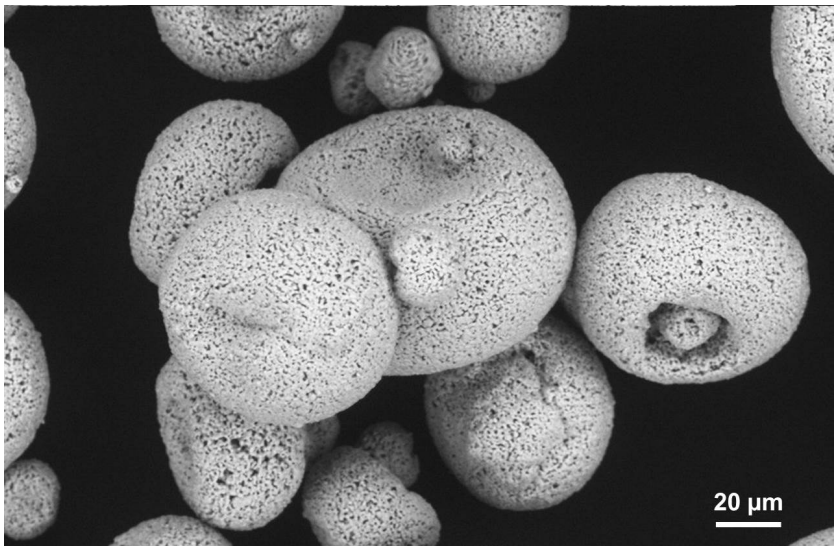

Figure 4. SEM picture showing the surface morphology of ceramic $La_2Zr_2O_7$ particles.

Figure 5 shows the external morphology of the nanostructured ZrO_2-$7Y_2O_3$ agglomerates, that have to be partially melted in order to restrain part of the starting nanostructure in the final coating. The external surface of these agglomerates typically exhibits complete melting, whereas the particle core usually remains un-melted or in semi-molten state, thus partially preventing the grain growth, depending on the high temperature experienced during processing as well as on the dwell time of the melted droplets in the plasma jet. Similar morphology can be observed for nanostructured WC-Co particles (see Fig. 6), where WC particles are cemented by a metallic binder phase that allows to restrict the effects of decarburization during processing and to retain good toughness in the resulting composite coating.

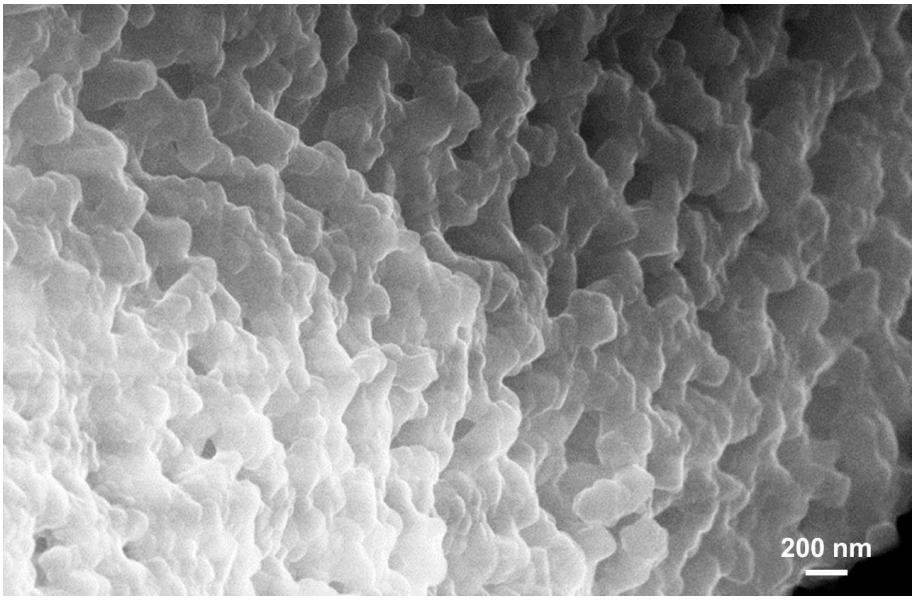

Figure 5. SEM picture showing nanoparticles on the surface of ZrO_2-$7Y_2O_3$ agglomerates.

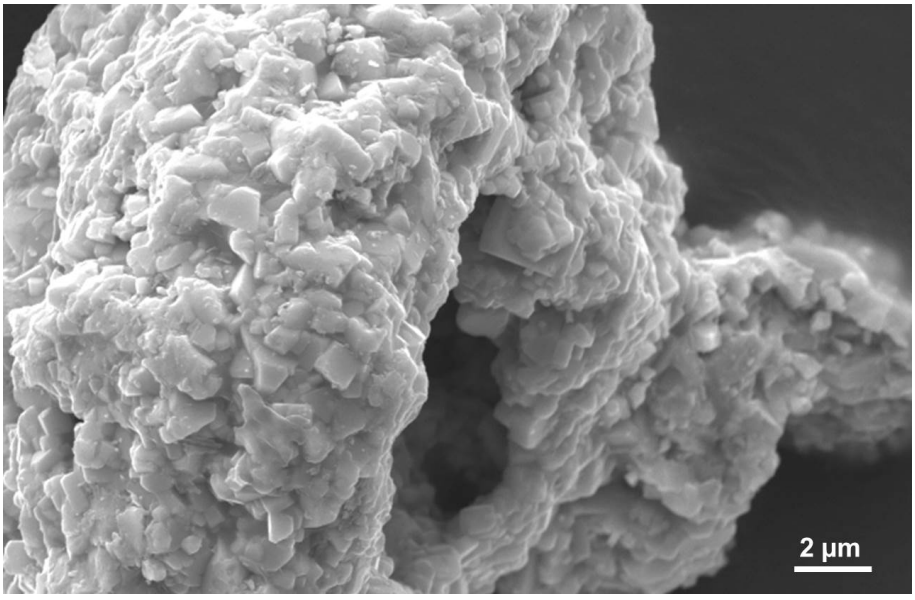

Figure 6. SEM picture showing an agglomerate of WC-Co nanoparticles.

3. Sample Preparation

The coatings were deposited on Ni-superalloy substrates (Φ = 25 mm, t = 5 mm) using an APS system equipped with F4-MB plasma torch with 6 mm internal diameter nozzle (Sulzer Metco, Wolhen, Switzerland). The following powder feedstock are used: a) 88WC-12Co (Infralloy S7412, Inframat, North Haven, CT) composed of agglomerates with diameter in the range 10–100 μm; b) ZrO_2-7Y_2O_3 (Nanox S4007, Inframat Corporation, North Haven, CT) with agglomerates of 15–150 μm in diameter; c) CoNiCrAlYRe (52Ni10Co24Cr10Al1Y3Re, Sicoat 2453, Siemens AG, Mulheim, Germany) with particles in the range 46–66 μm; d) $La_2Zr_2O_7$ (43 wt.% ZrO_2–57 wt.% La_2O_3, Trans-Tech Inc, Adamstown, MD) with particles in the range 37–149 μm. The substrates were sand blasted with alumina abrasive powder to increase their surface roughness, then cleaned and coated. The deposited thickness was set to 300 μm for all the coating systems. The plasma spraying parameters used to produce the coatings were reported in previous papers [21,25,26,27]. Powder morphology and coating microstructure were analyzed using a SEM-FEG (Scanning Electron Microscope-Field Emission Gun, Leo Gemini mod. 1530 Carl Zeiss, Oberkochen, Germany) equipped with high-resolution secondary (in-lens), secondary electron (SE) and back scattered electron (BSE) detectors as well as with electron dispersive spectroscopy (EDS) detector.

The analysis of the microstructural defects of thermally sprayed coatings required proper preparation of the samples. The samples were cut by low-speed diamond saw and their cross sections were cold mounted in vacuum in two-part polymer, ground and polished to 0.25 μm. Hot compression mounting is not recommended as the molding pressure can collapse the typical voids embedded in thermally sprayed coatings. On the contrary, the use of low-viscosity castable epoxy and vacuum infiltration allowed to fill the connected voids with epoxy, also making it easier to keep the pore walls flat to the edge during preparation, thus avoiding effects of pull-out, smearing, delamination and edge rounding.

4. Processing and Microstructure

Scanning Electron Microscopy is an advanced powerful technique suitable to investigate the main morphological and microstructural characteristics of materials and coatings. The current expertise allows us to develop ad-hoc analyses as well as to extend the methodology to a high variety of materials and case studies.

Figure 7 shows the cross sectional microstructure of a CoNiCrAlYRe coating deposited on the surface of Ni-superalloy substrate. The metallic coating is characterised by a lamellar microstructure composed of melted splats and embedding a network of typical defects, such as splat boundaries, microcracks and pores.

Splat boundaries are produced by weak bonding and filling defects between overlapped deposited splats. Indeed, the melted particles impact on the surface of previously deposited splats, that are previously solidified and cooled down, and are flattened. In turn, microcracks result from release of thermal stresses during fast cooling of the deposited splats at room temperature. Globular pores derive from gas entrapped in the molten droplets partly solidified before their impacting on the substrate, while pores with larger size typically result from filling defects during spreading of impacting particles and pull-out effects occurring during polishing [28,29].

Splat boundaries are areas more prone to oxidation and growth of oxides during processing of metal particles, because the external surface of the sprayed particles is in contact with the

surrounding oxidizing environment. These zones are also more susceptible to further selective oxidation during high-temperature exposure in turbine real operative environment.

As shown in Fig. 7, the CoNiCrAlYRe coating is characterised by two-phase structure, composed by light gray γ phase and embedded dark gray β phase-rich precipitates. These dark areas are more rich of Al and Ni in comparison with the matrix: the amount of Al can be directly related to the oxidation resistance of the particles during spraying. When the oxidation takes place, the precipitates are subjected to Al diffusion through gas infiltration mechanism, especially at the external surface of the sprayed particles or melted splats, so that the retained Al content can be rightly considered as a reservoir for selective oxidation as well as a measure of the oxidation resistance of the coating [30,31]. At the same time, these precipitates can experience some effects of coalescence depending on the cooling rate experienced during splat solidification at the substrate surface.

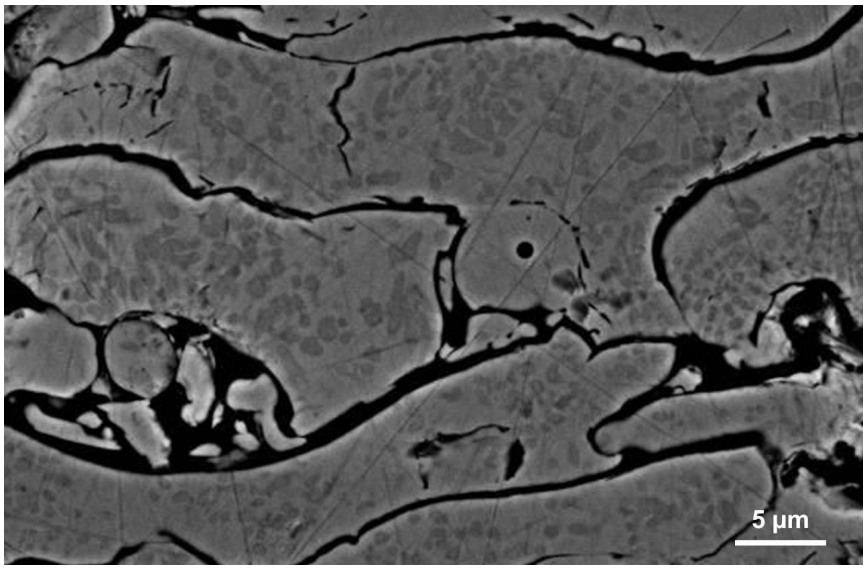

Figure 7. SEM picture showing the cross sectional microstructure of CoNiCrAlYRe coating.

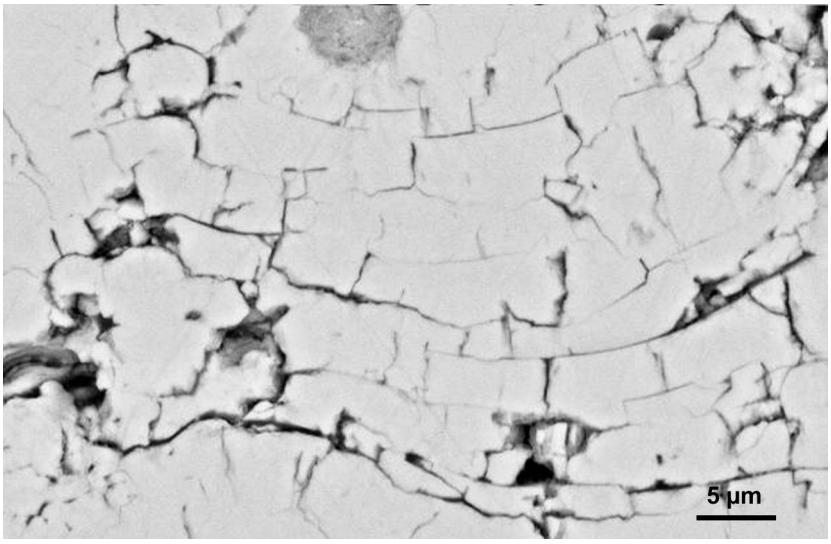

Figure 8. SEM picture showing the cross sectional microstructure of $La_2Zr_2O_7$ coating.

Figure 8 shows the cross sectional microstructure of plasma sprayed $La_2Zr_2O_7$ coating characterised by typical defects such as splat boundaries, pores with different shape and size, and vertical microcracks. Microcracks are herein more visible because of the high thermal stresses produced during quenching and solidification of the deposited melted splats at the substrate surface. The presence of splat boundaries is able to significantly reduce the thermal conductivity of the coating, thus increasing the thermal insulation of the underlying component. However, it also reduces the inter-lamellar bonding strength. All these defects contribute to the total porosity of the coating and then to the values of thermal and mechanical properties, such as thermal conductivity, microhardness and Young's modulus. Many studies have demonstrated that quantitative microstructural investigation by image analysis techniques allows to calculate the amount of the total porosity as well as to identify and quantify pores and cracks with various shape and size [7,8]. Obviously, it is worth noting that image analysis requires reliable and reproducible cross sectional images and can be affected by image acquisition conditions and threshold selection for pore identification.

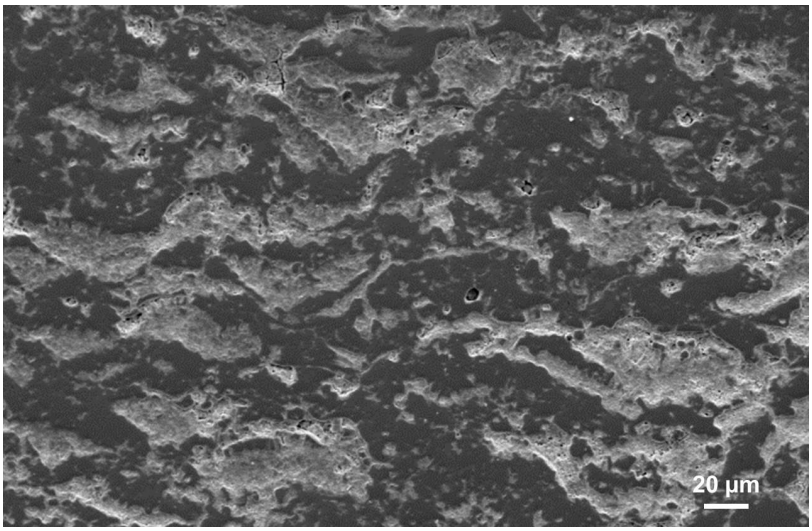

Figure 9. SEM picture showing the bimodal microstructure of nanostructured ZrO_2-$7Y_2O_3$ coating cross section.

Scanning electron microscopy can be also addressed to detailed investigation of the nanostructured features of ceramic coatings deposited by plasma spraying. Figure 9 shows the cross sectional microstructure of nanostructured zirconia-yttria coating. By controlling the degree of melting of the nanostructured agglomerates it is possible to retain part of the starting nanostructure and to obtain a coating with a typical "bimodal" microstructure, where the semi-molten areas, consisting of loosely bounded nanostructured particles (see Fig. 10) and resembling the morphology of the starting nanoparticles, are uniformly distributed along coating thickness and are cemented by the melted areas that act as a binder phase, ensuring the mechanical integrity of the coating. The melted areas are characterised by overlapped lamellae with embedded columnar grains, oriented along the direction of grain growth and surrounded by any equiaxed grains located at splat boundary, as detectable in the fractured cross section displayed in Fig. 11. The former are produced by heterogeneous nucleation at splat boundary and their growth into the molten splat, because of heat flow released by crystallization of previously deposited splats: their size is between tens and

hundreds of nanometers. In turn, the latter are originated by homogeneous nucleation effect [32]. Low heat transfer associated to the intrinsic porosity of the ceramic agglomerates and high quenching rate of the solidified droplets are both factors able to reduce the grain growth.

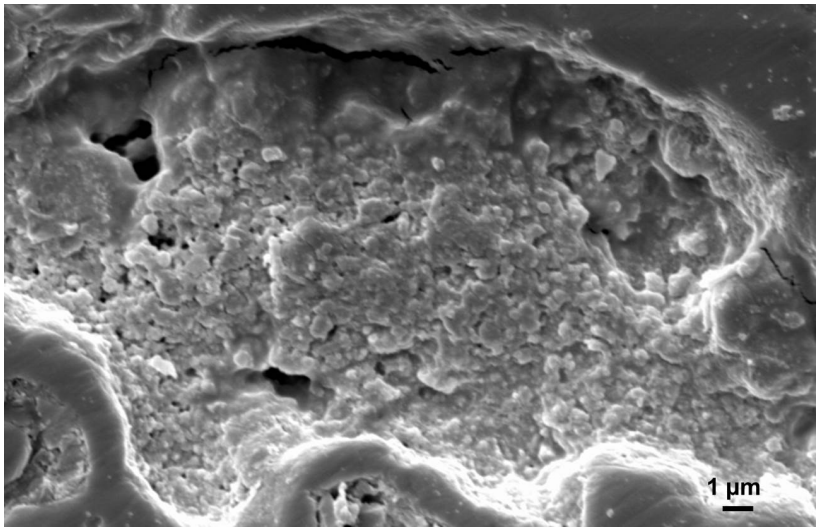

Figure 10. SEM picture showing the detail of some un-melted areas, characterised by presence of loosely bounded particles (coating cross section).

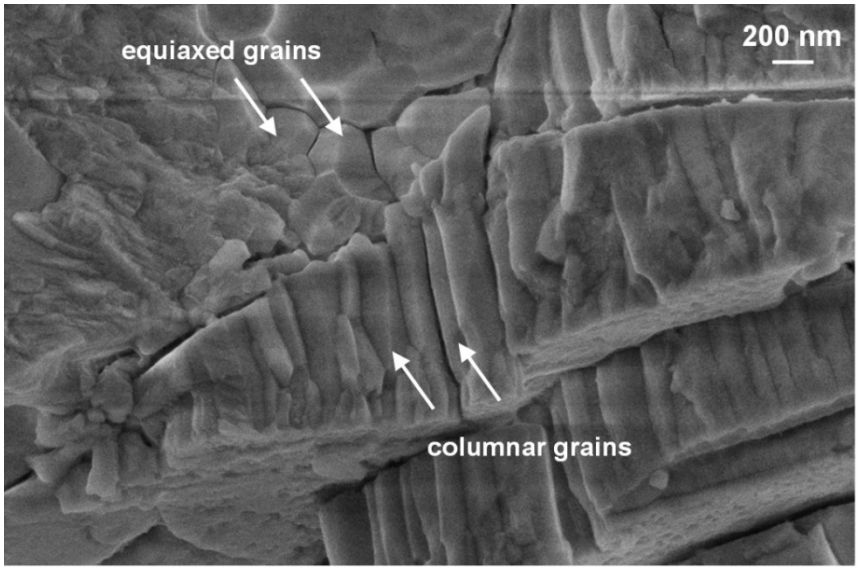

Figure 11. SEM picture showing the lamellar microstructure of nanostructured zirconia-yttria coating fractured cross section with embedded columnar and equiaxed grains. Reprinted with permission from [32], Di Girolamo G, Marra F, Blasi C, et al. (2010) Microstructure, mechanical properties and thermal shock resistance of plasma sprayed nanostructured zirconia coatings. *Ceram Int* 37: 2711-2717, © 2010, Elsevier.

Some particles are heated at lower rate and are subjected to grain growth. As they impinge on the substrate as they produce the formation of a smooth surface with embedded microcracks, as well observable in Fig. 12. The content of fully melted areas should be restricted to certain extent, in order

to reach the best compromise between the structural integrity and the retention of nanostructured areas in the coating system.

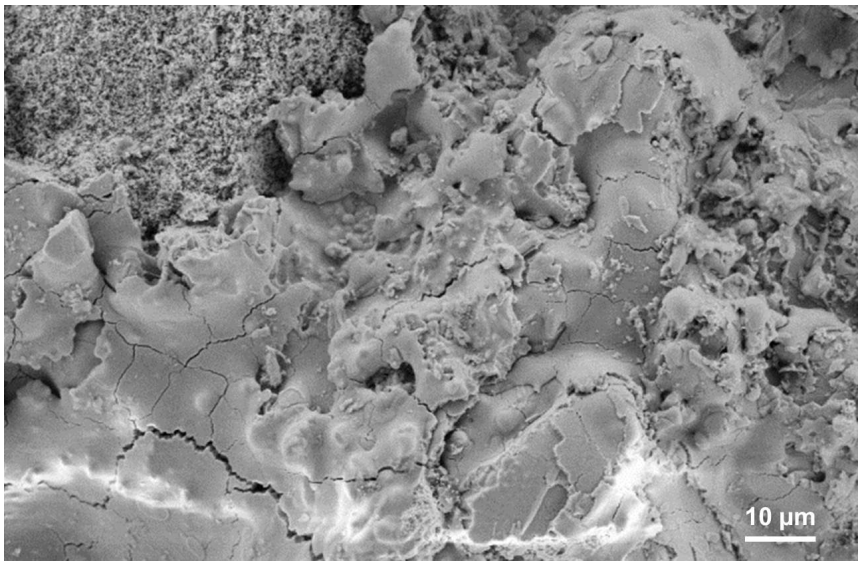

Figure 12. SEM picture showing the plan surface morphology of the nanostructured zirconia-yttria coating.

Coatings with tailored microstructure for well-determined applications can be then easily manufactured, by controlling the porosity level, and thus their thermal and tribological properties. The presence of nanostructured semi-molten areas is recognized to be a positive factor for increasing the fracture toughness [25,33]. Indeed, these porous regions are able to arrest the propagation of microcracks arising within the dense areas owing to thermal stresses release, as shown in Fig. 13 [33]. The bimodal microstructure generally involves a bimodal distribution of the mechanical properties [25].

Provided their unique properties, these coatings are suitable to be used for different applications, *i.e.* as thermal barriers, abradable coatings and so on, depending on the amount of the nanostructured areas they retain. Thermal barriers usually require high porosity (higher than 10%) but at the same time they have to ensure good insulation from corrosive media infiltration, as well as mechanical and cohesive strength. High porosity is surely able to improve the strain tolerance, the sintering resistance and the thermal insulation property. On the contrary, more friable abradable coatings require lower mechanical strength and then can tolerate very high value of porosity [34]. Previous works reported that quantitative image analysis of nanostructured YSZ coating SEM cross sections can be successfully performed in order to calculate the amount of retained nanostructured areas as well as porosity value and distribution [25,35].

Nanostructured coatings can be also used for anti-wear applications. This is the case of carbide-based coatings (WC-Co, Cr_2C_3 and so on), that are commonly adopted to protect fan blades and flanges of jet engine parts, rocker arms, piston rings, cylinder lines, compressor air seals and valve seats, dovetail interlocks, discs, shafts, casings and nozzle wear pads of gas turbines [36,37,38]. They are generally used in cold sections, because their tribological properties dramatically drop as the temperature increases, because of the thermal decomposition and the following formation of secondary and ternary carbides, both typically characterised by high hardness and brittleness.

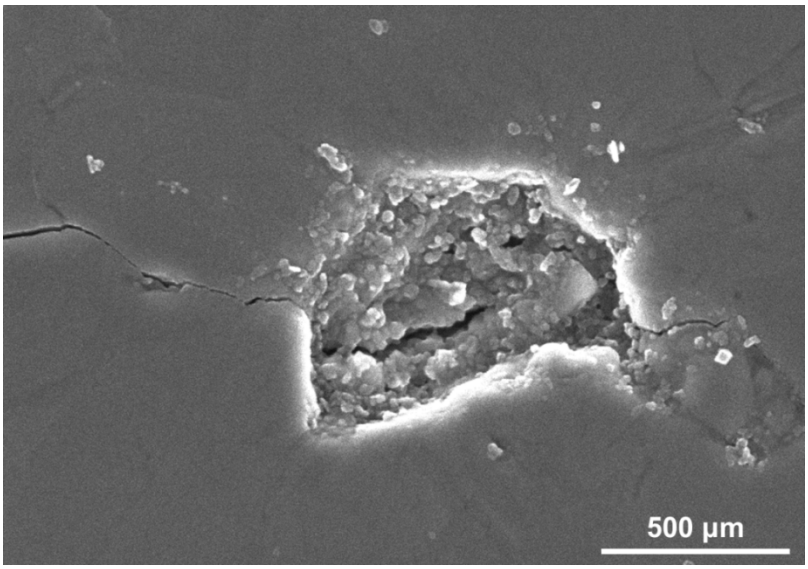

Figure 13. Vickers indentation crack tip arresting after passing through a nanozone in the nanostructured coating (coating cross section). Reprinted with permission from [33], Lima RS, Marple BR (2007) Thermal spray coatings engineered from nanostructured ceramic agglomerated powders for structural, thermal barrier and biomedical applications: a review. *J Therm Spray Technol*, 16: 40–63, © 2007, Springer.

The thermal effects during processing of carbide powder particles have to be restricted, in order to reduce any effects of decomposition and unacceptable reduction of mechanical and tribological performance.

Indeed, it is well known that during processing some chemical reactions occur in the plasma core and take place during the flight of the molten droplets and their quenching at the substrate surface [39]. Both high temperature and oxidizing environment can affect the final composition of the coating, promoting some effects of carbide decomposition in the metal matrix and decarburization, which result in the growth of undesired brittle secondary and ternary carbides, in crystalline or amorphous form, as observable in Fig. 14: the XRD pattern of nanostructured WC-Co coating surface deposited by plasma spraying demonstrates the formation of new crystalline phases (α-W_2C, β-WC_{1-x} and $Co_xW_yC_z$) as well as the formation of a mixed amorphous phase, represented by two broad humps in the pattern, for $35° < 2\theta < 45°$ and $72° < 2\theta < 80°$, respectively. Secondary and ternary carbides are typically characterised by high hardness and low toughness, so that their presence can negatively affect the tribological behaviour. In order to reduce the degree of decarburization it is necessary to use processes and gas mixtures able to reduce the particle temperature as well as to increase the particle speed, thus significantly reducing the residence time of the sprayed particles in the flame or plasma jet.

The SEM picture reported in Fig. 15 shows that the nanostructured WC-Co coating is composed of WC nanograins homogeneously dispersed in the binder phase. The different stage of coalescence of the grains is associated to the history of the melted particles depending on the temperature distribution in the plasma jet. Some strip- and square-shaped structures, approximately in the range between 500 nm and 1 µm, probably derive from a second recrystallization during successive torch passes. The carbide grains which are partially dissolved and mixed with the Co-matrix produce ultrafine Co-rich dendritic structures.

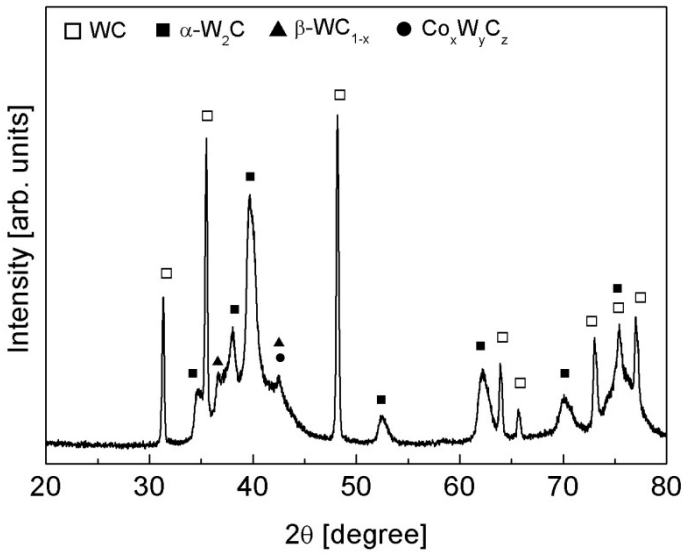

Figure 14. XRD pattern of plasma sprayed nanostructured WC-Co coating.

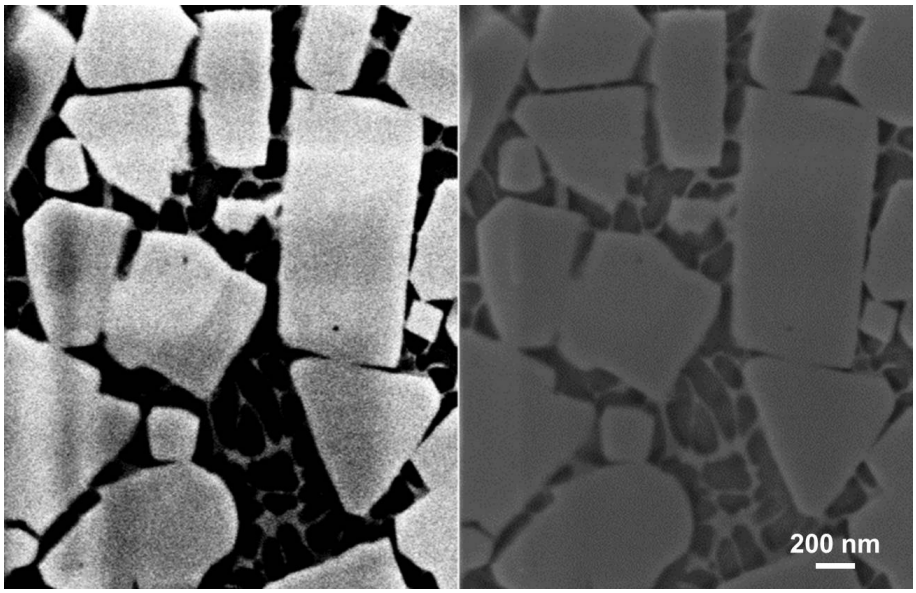

Figure 15. SEM picture showing some microstructural features of nanostructured WC-Co coating cross section. WC grains are herein dispersed in the binder phase (SE and BSE pictures).

In conclusion, the effects of carbide decomposition and grain growth have to be properly restrained to produce high-quality coatings, since the wear resistance decreases with increasing the degree of decarburization of carbide particles.

5. Effects of Aging on the Microstructure of Metallic and Ceramic Coatings

Scanning electron microscopy and EDS can be also successfully employed to investigate and analyze in detail the effects promoted by thermal exposure on metallic and ceramic coatings. Figure

16 shows the cross sectional microstructure of porous CoNiCrAlYRe coating exposed at 1100 °C for 50 h and subjected to severe oxidation. Generally, the diffusion of Al from the β precipitates promotes the growth of an alumina rich scale that partially inhibits the quick formation of brittle secondary oxidation products. As shown in the EDS map reported in Fig. 17, a quasi-continuous, uniform and dense dark grey alumina scale usually surrounds pores and splat boundaries and, in any cases, is partially covered by an upper thin and irregular mixed grey oxide scale, that being an undesirable product in terms of structural integrity and oxidation durability [40].

The rough top-surface and the existence of pores and splat boundaries represent preferential pathways for oxygen infiltration and assist the environmental attack and the internal oxidation of the coating. High temperature produces some effects of sintering, but in localized areas preferential paths for oxygen propagation allow oxygen diffusion and its reaction with Al, thus leading to Al depletion and fast growth of secondary oxide scales, such as Al_2O_3 (dark grey phase in Fig. 16), spinels (medium grey phase, mainly composed of Ni, Cr and O), NiO (light grey phase), Cr_2O_3, as well detectable in the XRD patterns reported in Fig. 18. By comparing the XRD results with the SEM-EDS maps it is possible to identify the distribution and the composition of all the phases within the microstructure.

These mixed oxide scales are characterised by high brittleness and tendency to delamination, so that they are preferential sites for localized stresses and crack nucleation [41]. This reduces the insulation against further oxygen propagation and the cohesive strength within the coating and at the top surface. This last issue is problematic in all the applications where the surface of the metal is then furtherly coated by a ceramic TBC which, in that case, will be able to detach or spall from the underlying metal, because of the gradual volume increase, horizontal cracking and loss of adhesion/mechanical interlocking.

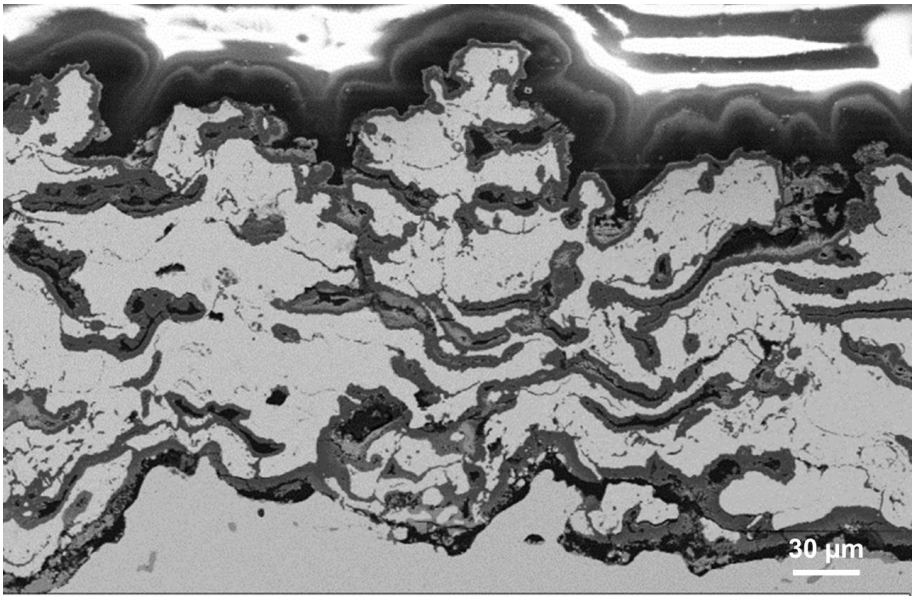

Figure 16. SEM picture showing the cross sectional microstucture of CoNiCrAlYRe coating exposed at 1100 °C and largely oxidized.

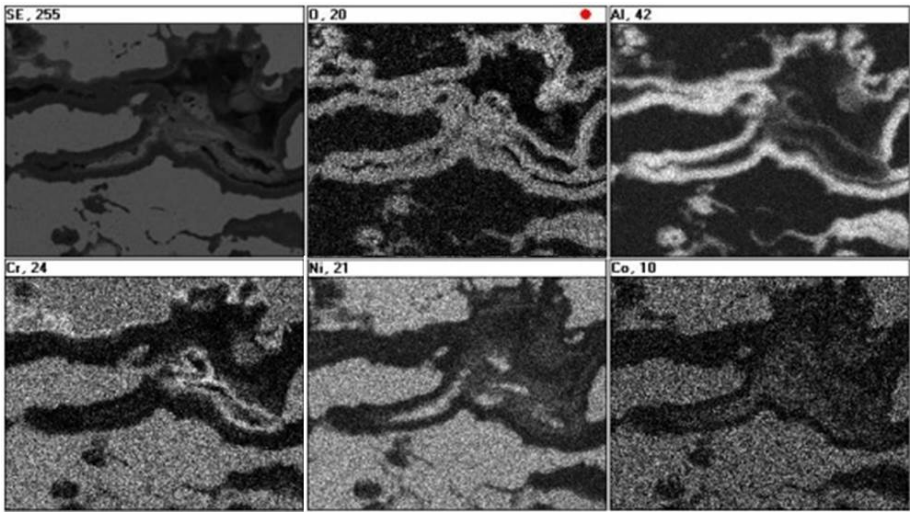

Figure 17. EDS map showing the growth of oxide scales at splat boundary within the oxidized coating cross section.

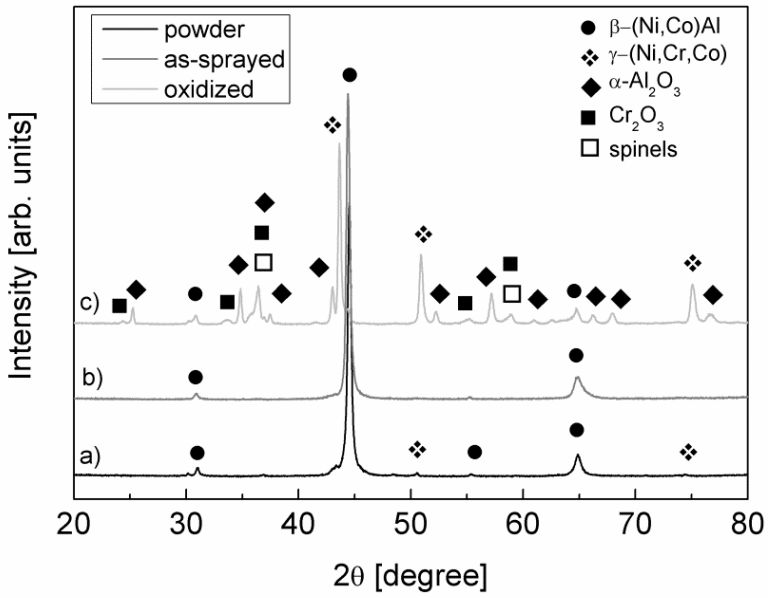

Figure 18. XRD pattern of CoNiCrAlYRe a) powder, b) as-sprayed and c) oxidized coating surface. Reprinted with permission from [21], Di Girolamo G, Brentari A, Blasi C, et al (2014) High-temperature oxidation and oxide scale formation in plasma-sprayed CoNiCrAlYRe coatings. *Metall Mater Trans* 45A: 5362–5370, © 2014, Springer.

EDS analysis also highlights that the Cr depletion is more pronounced in the areas characterised by higher oxidation rate. The outward diffusion of Ni and Cr and their reaction with oxygen lead to the growth of spinels ($NiCr_2O_4$, $NiAl_2O_4$, and so on), by reaction between Cr_2O_3 (and Al_2O_3) and NiO. The growth of secondary oxide phases generally occurs in restricted areas where more pronounced Al depletion does not allow the formation of a stable and protective Al_2O_3 layer, whereas it is less significant in the areas characterised by growth of a continuous and well-adherent

alumina scale. The EDS map reported in Fig. 17 shows the dispersion of the elements on the oxidized surface of CoNiCrAlYRe coating exposed at 1100 °C for 50 h. Light grey particles are mostly composed of spinels and Cr_2O_3.

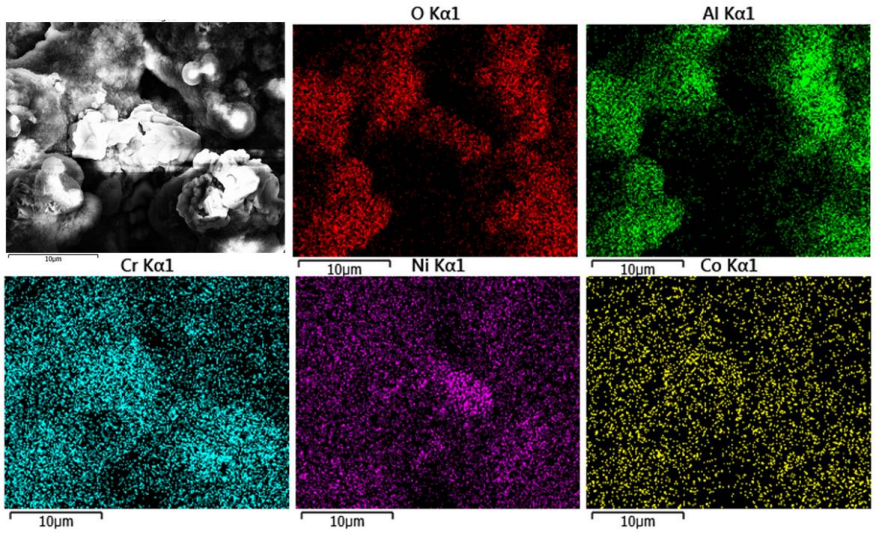

Figure 17. EDS map showing the dispersion of the elements on the oxidized plan surface of CoNiCrAlYRe coating exposed at 1100 °C for 50 h.

Microstructural investigation by scanning electron microscopy also allows to obtain key information about any common effects of thermal aging occurring in ceramic thermal barrier coatings working at very high temperature (1200 °C and higher). The sintering effects, in addition to phase changes, thermal stresses arising from oxidation of metal surface and CTE mismatch between metal and ceramic, and delamination by corrosion, are one of the main factors affecting the performance and the durability of porous thermal barrier coatings applied on metal components of hot sections operating in turbine engines [42,43,44]. As shown in Figs. 18 and 19, after thermal exposure at 1350 °C for 50 h, some effects of sintering are visible in the cross section of $La_2Zr_2O_7$ thermal barrier coating. By diffusion mechanism the heat treatment at high temperature assists the partial closure of fine pores and splat boundaries embedded in the coating microstructure, leading to the formation of sintering necks. Fine microcracks and splat boundaries tend to disappear, whereas the large pores are subjected to the mechanism of densification at lesser extent. Therefore, the nature of pores and interfaces, their shape and size, play a key role on the sintering behaviour of plasma sprayed coatings. Generally, during the first hours of laboratory heat treatment or service operation, the formation of sintering necks between the lamellae reduces the inter-lamellar porosity, so that it is difficult to distinguish the original lamellar microstructure, whereas as the time increases as the sintering rate tends to decrease. Nevertheless the coating continues to densify at lesser extent.

Sintering mechanism takes place by a reduction of the total porosity of the coating, thus increasing both its stiffness and hardness [43]. However, it reduces the strain tolerance of the same coating that will be less able to accomplish the thermal stresses arising during repeated heating and cooling cycles experienced by the coated component during service [45,46]. This dramatically increases the risk for cracking, delamination and spallation, thus leading to the progressive damage of the whole TBC system. At this purpose, it has been also reported that under high-temperature

mechanical load (high–temperature bending test) these coatings exhibit inelastic deformation and stress relaxation, associated to the sliding of their weakly bonded splat boundaries and to the propagation/deflection of the embedded microcracks: both these effects are able to counteract the gradual sintering of the microstructure [27].

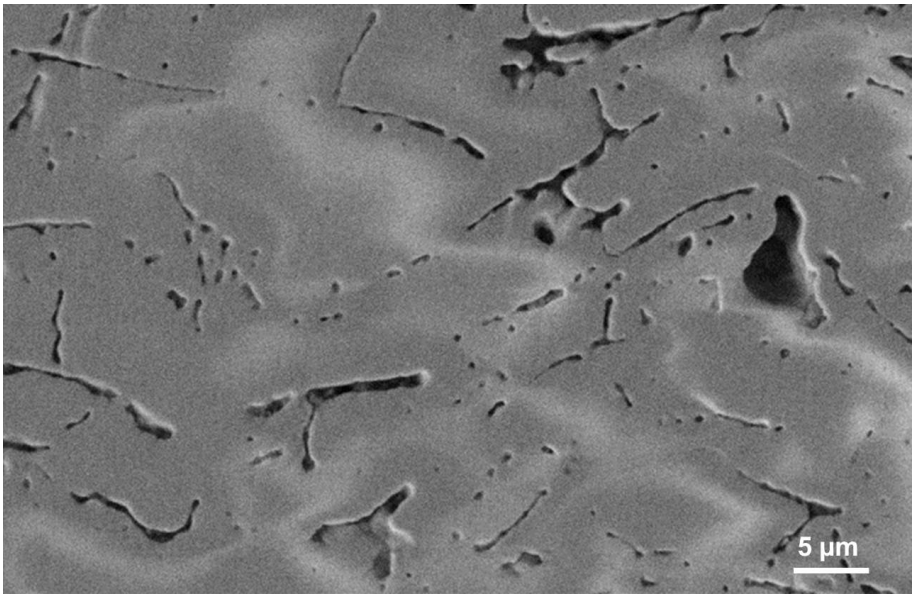

Figure 18. SEM picture showing the cross sectional microstructure of aged $La_2Zr_2O_7$ coating. Some effects of sintering (closure of pores and formation of sintering necks) are detectable.

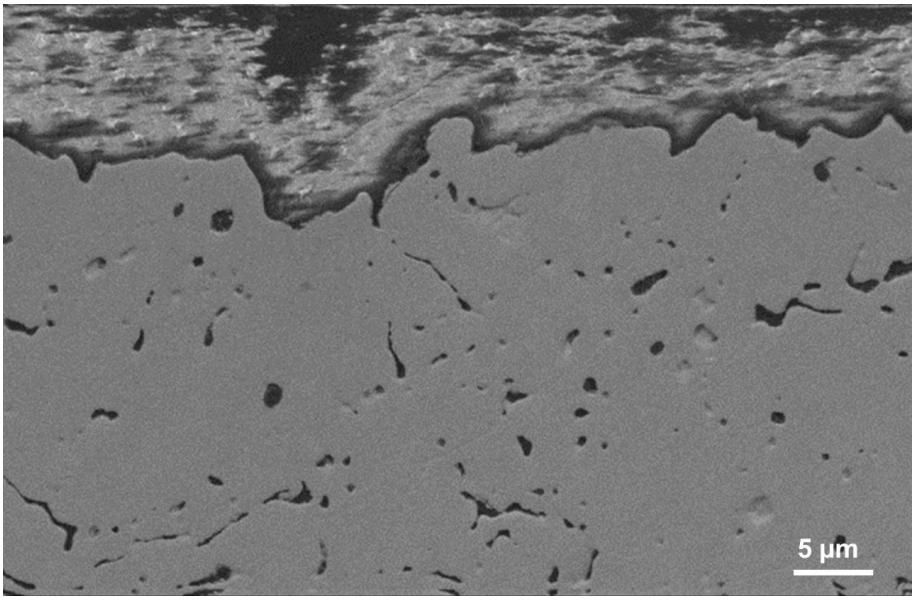

Figure 19. SEM picture showing the cross sectional microstructure of aged $La_2Zr_2O_7$ coating cross section. The lamellar microstructure tends to disappear after thermal exposure.

In conclusion, this work reports a large and useful overview on selected microstructural characterisation examples of plasma sprayed coatings, suggesting valuable methodologies and good perspectives for further development of characterisation techniques and material optimization, adaptable to a wide variety of materials for a wide range of applications and components working at extreme service conditions. This implies potential future directions the investigators can focus their attention to, for their research purposes in material science as well as for supporting designers, manufacturers and end-users of related industrial components.

6. Conclusion

Microstructural analysis is a powerful tool enabling the investigation of the main characteristics and the mechanisms affecting the functional properties of porous materials and coatings (metallic, ceramic, composite) addressed to various industrial applications. Thermal spray processing of powder-based particles usually produces coatings with unique microstructure, whose particular features and defects, such as pores, splat boundaries and cracks at micro and nano scale, can be successfully detected and analyzed using advanced microstructural characterisation, and mainly SEM-EDS technique. Therefore, the relationship between processing and microstructure as well as the relationship between microstructure and operative behaviour/performance can be properly investigated and assessed. The effects of thermal aging on the microstructural evolution of coatings manufactured by plasma spraying can be also investigated by SEM analyses: morphological, microstructural and compositional modifications, quantitative and qualitative evaluation of high-temperature densification, crack nucleation and propagation, grain growth, growth of oxide scale, delamination are examples of typical details that can be clearly detected and analyzed in order to obtain useful information about the state of the related component, its environmental resistance and long-term durability.

Acknowledgments

The authors wish to thank Caterina Blasi for her valuable support in plasma spraying trials.

Conflict of Interest

All authors declare no conflict of interest in this paper.

References

1. Davis JR (2004) In: Coutsouranis D (Ed.), Handbook of thermal spray technology. *ASM International*, Materials Park, OH.
2. National Research Council (1996) Coatings for high-temperature applications: trends and opportunities. *National Academy of Sciences*, Washington DC.
3. Zhou D, Miller RA (2002) Thermal conductivity and sintering behaviour of advanced thermal barrier coatings, *26th Annual Conference on Advanced Ceramics and Composites, American Ceramic Society*. Cocoa Beach, Florida, January 13–18.
4. Hutchinson JW, Evans AG (2002) On the delamination of thermal barrier coating in a thermal gradient. *Surf Coat Technol* 149: 179–184.

5. Evans AG, Mumm DR, Hutchinson JW, et al. (2001) Mechanisms controlling the durability of thermal barrier coatings. *Progress Mater Sci* 46: 505–553.
6. Amsellen O, Borit F, Jeulin D, et al. (2013) Best paper in journal of thermal spray technology: 3D analysis in microstructure of thermal spray coatings. *Metallogr Microstruct Anal* 2: 196–201.
7. Kulkarni AA, Goland A, Herma H, et al. (2004) Advanced microstructural characterization of plasma-sprayed zirconia coatings over extended length scales. *J Therm Spray Technol* 14: 239–250.
8. Juzkova R, Ctibor P, Benes V (2004) Analysis of porous structure in plasma-sprayed coating. *Image Anal Stereol* 23: 45–52.
9. Zhao Y, Shinmi A, Zhao X, et al. (2012) Investigation of interfacial properties of atmospheric plasma sprayed thermal barrier coatings with four-point bending and computed tomography technique. *Surf Coat Technol* 206: 4922–4929.
10. Espargallas N (Ed.) (2015) Future development of thermal spray coatings. Types, design, manufacture and applications (2015) *Woodhead Publishing*.
11. Cetegen BM, Yu W (1999) In-situ particle temperature, velocity and size measurements in DC arc plasma thermal sprays. *J Therm Spray Technol* 8: 57–67.
12. Qiao Y, Fischer TE, Dent A (2003) The effect of fuel chemistry and feedstock powder on the mechanical and tribological properties of HVOF thermal-sprayed WC-Co coatings with very fine structures. *Surf Coat Technol* 172: 24–41.
13. Singh H, Sidu TS, Kalsi SBS (2012) Cold spray technology: future of coating deposition processes. *Frattura ed Integrità Strutturale* 22: 69–84.
14. Moridi A, Hassani-Gangaraj SM, Guagliano M, et al. (2014) Cold spray coating: review of material systems and future perspectives. *Surf Eng* 36:369–395.
15. Morsi MS, Abd El Gwad SA, Shoeib MA, et al. (2012) Effect of air plasma sprays parameters on coating performance in zirconia-based thermal barrier coatings. *Int J Electrochem Sci* 7: 2811–2831.
16. Chen Z, Yuan F, Wang Z, et al. (2007) The oxide scale formation and evolution on detonation gun sprayed NiCrAlY coatings during isothermal oxidation. *Mater Trans* 48: 2695–2702.
17. Curry N, Van Every K, Snyder T, et al. (2015) Performance testing of suspension plasma sprayed thermal barrier coatings produced with varied suspension parameters. *Coatings* 5: 338–356.
18. Wang C, Wang I, Wang L, et al (2014) Nanocomposite lanthanum zirconate thermal barrier coating deposited by suspension plasma spray process. *J Therm Spray Technol* 7: 1030–1036.
19. Jordan EH, Xie L, Gell M, et al. (2004) Superior thermal barrier coating using solution precursor plasma spray. *J Therm Spray Technol* 13: 57–65.
20. Yuan J, Zhan Q, Huang J, et al. (2013) Dercaburization mechanisms of WC-Co during thermal spraying: insights from controlled carbon loss and microstructure characterisation. *Mater Chem Phys* 142: 165–171.
21. Di Girolamo G, Brentari A, Blasi C, et al. (2014) High-temperature oxidation and oxide scale formation in plasma-sprayed CoNiCrAlYRe coatings. *Metall Mater Trans* 45A: 5362–5370.
22. He J, Schoenung JM (2002) Nanostructured coatings. *Mater Sci Eng A* 336: 274–319.
23. Gell M, Jordan EH, Sohn YH, et al. (2001) Development and implementation of plasma sprayed nanostructured ceramic coatings. *Surf Coat Technol* 146–147: 48–54.
24. Shaw LL, Goberman D, Ren R, et al. (2000) The dependency of microstructure and properties of nanostructured coatings on plasma spray conditions. *Surf Coat Technol* 130: 1–8.

25. Lamuta C, Di Girolamo G, Pagnotta L (2015) Microstructural, mechanical and tribological properties of nanostructured YSZ coatings produced with different APS process parameters. *Ceram Int* 41: 8904–8914.
26. Di Girolamo G, Marra F, Pilloni L, et al. (2013) Microstructure and wear behaviour of plasma sprayed nanostructured WC-Co coatings. *Int J Appl Ceram Technol* 10: 60–71.
27. Di Girolamo G, Marra F, Schioppa M, et al. (2015) Evolution of microstructural and mechanical properties of lanthanum zirconate thermal barrier coatings at high temperature. *Surf Coat Technol* 268: 298–302.
28. Bengtsson P, Johannesson T (1995) Characterisation of microstructural defects in plasma-sprayed thermal barrier coatings. *J Therm Spray Technol* 4: 245–251.
29. Nakamura T, Qian G, Berndt CC (2000) Effects of pores on mechanical properties of plasma-sprayed ceramic coating. *J Am Ceram Soc* 83: 578–584.
30. Shibata M, Kuroda S, Muramaki H, et al. (2006) Comparison of microstructure and oxidation behaviour of CoNiCrAlY bond coatings prepared by different thermal spray processes. *Mater Trans* 47:1638–1642.
31. Fossati A, Di Ferdinando M, Lavacchi A, et al. (2011) Improvement of the oxidation resistance of CoNiCrAlY bond coats sprayed by high velocity oxygen-fuel onto nickel superalloy substrate. *Coatings* 1: 3–16.
32. Di Girolamo G, Marra F, Blasi C, et al. (2010) Microstructure, mechanical properties and thermal shock resistance of plasma sprayed nanostructured zirconia coatings. *Ceram Int* 37: 2711–2717.
33. Lima RS, Marple BR (2007) Thermal spray coatings engineered from nanostructured ceramic agglomerated powders for structural, thermal barrier and biomedical applications: a review. *J Therm Spray Technol* 16: 40–63.
34. Lima RS, Marple BR (2006) Nanostructured abradable coatings for high temperature applications. *Thermal Spray 2006: proceedings of the International Thermal Spray Conference*. May 15-18, Seattle, Washington, 775–780.
35. Lima RS, Kucuk A, Berndt CC (2002) Bimodal distribution of mechanical properties on plasma sprayed nanostructured partially stabilized zirconia. *Mater Sci Eng A* 327: 224–232.
36. Sanchez E, Bannier E, Salvador MD, et al. (2010) Microstructure and wear behaviour of conventional and nanostructured plasma-sprayed WC-Co coatings. *J Therm Spray Technol* 19: 964–974.
37. Zhao XQ, Zhou HD, Chen JM (2006) Comparative study of the friction and wear behaviour of plasma sprayed conventional and nanostructured WC-12%Co coatings on stainless steel. *Mater Sci Eng A* 431: 290–297.
38. Shipway PH, McChartney DG, Sudaprasert T (2005) Sliding wear behaviour of conventional and nanostructured HVOF sprayed WC-Co coatings. *Wear* 259: 820–827.
39. Di Girolamo G, Pilloni L, Marra F, et al. (2009) Tribological characterisation of WC-Co plasma sprayed coatings. *J Am Ceram Soc* 92: 1118–1124.
40. Rabiei A, Evans AG (2000) Failure mechanisms associated with the thermally grown oxide in plasma-sprayed thermal barrier coatings. *Acta Mater* 48: 3963–3976.
41. Keyvani A, Saremi M, Heydarzadeh SM (2011) Oxidation resistance of YSZ-alumina composites compared to normal YSZ TBC coatings at 1100 °C. *J Alloys Compd* 509: 8370–8377.
42. Lima RS, Marple BR (2008) Nanostructured YSZ thermal barrier coatings engineered to counteract sintering effects. *Mater Sci Eng A* 485: 182–193.

43. Alfano M, Di Girolamo G, Pagnotta L, et al. (2010) The influence of high temperature sintering on microstructure and mechanical properties of APS CeO_2-Y_2O_3-ZrO_2 coatings. *J Mater Sci* 45: 2662–2669.
44. Chen H, Gao Y, Tao S, et al. (2009) Thermophysical properties of lanthanum zirconate coating prepared by plasma spraying and the influence of post-annealing. *J Alloys Compd* 486: 391–399.
45. Haynes JA, Ferber MK, Porter WD (2000) Thermal cycling behaviour of plasma-sprayed thermal barrier coatings with various MCrAlX bond coats. *J Therm Spray Technol* 9: 38–48.
46. Liang B, Ding C (2005) Thermal shock resistance of nanostructured and conventional zirconia coatings deposited by atmospheric plasma spraying. *Surf Coat Technol* 197: 185–192.

AIMS Press